ON THE APPLICATION OF STOCHASTIC DECOMPOSITION IN THE ANALYSIS OF WIND EFFECTS

Xinzhong Chen and Ahsan Kareem

Department of Civil Engineering and Geological Sciences,
University of Notre Dame, Notre Dame, IN 46556-0767, USA

ABSTRACT

This paper presents the formulation and application of stochastic decomposition of covariance and cross-power spectral density matrices in the analysis of wind load effects on structures. This technique not only enhances our understanding of the underlying physics of wind loads and their effects on structures, but also provides efficient means to estimate structural response under multi-correlated excitations. Detailed discussion on the truncation of higher wind loading modes in the modeling and simulation of random wind load processes and associated analysis of wind effects are discussed using an example high-rise building.

KEYWORDS

Proper orthogonal decomposition, Stochastic decomposition, Simulation, Wind effects, Equivalent static load, Buildings, Random vibration, Turbulence.

INTRODUCTION

The stochastic decomposition scheme involves decomposition of the covariance and/or the cross-spectral density (XPSD) matrices of a multi-variate random process. This decomposition technique is theoretically based on the Karhunen-Loeve expansion which is also known as proper orthogonal decomposition (POD) or principal component analysis (PCA). Armit (1968) pioneered the application of POD of the covariance matrix to wind-related problems, and it was later used by many researchers in describing pressure fluctuations on buildings and structures and a host of wind-related problems (e.g., Lee 1975; Kareem 1978; Kareem and Cermak 1984; Holmes 1992; Davenport 1995; Carassale et al. 1998; Tamura et al. 1999; and Kareem 1999). The stochastic decomposition of fluctuating pressure field on a structure provides useful physical insight to the spatio-temporal nature of wind loads utilizing underlying eiegnvalues and eigenvectors. It also provides a useful means of relating the pressure field with the attendant load effects on structures.

The concept of stochastic decomposition of XPSD matrix as applied to probabilistic dynamics and digital simulation of multivariate random processes was introduced in Li and Kareem (1993 and 1995). It is very effective in determining the response of nested-cascade multiple input/output systems that require perturbation or iterative analysis techniques. It can also be useful in the dynamic analysis of large scale structures exposed to wind. Other applications can be found in Lin (1992), Di Paolo (1998), Carassale et al. (1998), Benfratello and Muscolino (1999), Kareem (1999) and Kareem and Mei (2000).

In this paper, the theoretical background of the stochastic decomposition technique is presented. Emphasis is placed on its application to the analysis of wind effects on structures. A detailed discussion on the truncation of higher wind loading modes in the modeling and simulation of random wind load processes and analysis of wind effects is provided using an example high-rise building.

STOCHASTIC DECOMPOSITION

Covariance Matrix

Following Mercier's theorem and the Karhunen-Loeve expansion, a discrete random field $\mathbf{p}(\mathbf{t}) = \{p(z_1, t), p(z_2, t), \ldots, p(z_N, t)\}^T$ can be expanded in terms of spatial optimal orthogonal matrix $\mathbf{\Phi}$ as:

$$\mathbf{p}(t) = \mathbf{\Phi a}(t) = \sum_{n=1}^{N} \mathbf{\Phi}_n a_n(t); \quad \mathbf{a}(t) = \mathbf{\Phi}^T \mathbf{p}(t) \tag{1}$$

The orthogonal matrix $\mathbf{\Phi}$ is the eigenvector matrix of the covariance matrix $\mathbf{R}_p$ with diagonal eigenvalue matrix $\mathbf{\Omega}$. These are given by:

$$\mathbf{R_p \Phi} = \mathbf{\Omega \Phi} \tag{2}$$

It is noted that the stochastic decomposition of the covariance matrix decomposes a set of correlated random processes $\mathbf{p}(t)$ into a number of component random sub-processes $\mathbf{a}(t)$. Any two random processes $a_i(t)$ and $a_j(t)$ are statistically non-correlated at zero time lag:

$$E[a_i(t)a_j(t)] = \delta_{ij} E[a_i^2(t)] = \delta_{ij}\Omega_i \tag{3}$$

It can be shown that the integral of the mean square value is equal to the sum of the eigenvalues, i.e.,

$$E[\mathbf{p}^T\mathbf{p}] = E[\mathbf{a}^T\mathbf{a}] = \sum_{n=1}^{N} E[a_n^2(t)] = \sum_{n=1}^{N} \Omega_n \tag{4}$$

In above, δ_{ij} is the Kroneker delta; and superscript T represents the matrix transpose operator.

Spectral Matrix

The XPSD matrix of random processes $\mathbf{p}(t)$ can be decomposed as:

$$\mathbf{S_p}(f) = \mathbf{D}(f)\mathbf{D}^*(f) \tag{5}$$

where $*$ represents transpose and conjugate operator. This decomposition can be obtained by the Cholesky or Schur (modal) decomposition. When the decomposition is based on the eigenvectors of XPSD matrix, $\mathbf{D}(f) = \mathbf{\Psi}(f)\sqrt{\mathbf{\Lambda}(f)}$, where $\mathbf{\Psi}(f)$ and $\mathbf{\Lambda}(f)$ are eigenvector and eigenvalue matrices, and given by:

$$\mathbf{S_p}(f)\mathbf{\Psi}(f) = \mathbf{\Lambda}(f)\mathbf{\Psi}(f) \tag{6}$$

The random processes $\mathbf{p}(t)$ can be viewed as the output of a system with a transfer matrix $\mathbf{\Psi}(f)$ and a vector-valued input $\mathbf{b}(t)$ with XPSD matrix of $\mathbf{\Lambda}(f)$, i.e.

$$\mathbf{p}(f) = \mathbf{\Psi}(f)\sqrt{\mathbf{\Lambda}(f)} = \mathbf{\Psi}(f)\mathbf{b}(f) = \sum_{n=1}^{N} \mathbf{\Psi}_n(f) b_n(f) \tag{7}$$

or it is written in the time domain as:

$$\mathbf{p}(t) = \sum_{n=1}^{N} \mathbf{p}_n(t); \quad \mathbf{p}_n(t) = \int_{-\infty}^{t} \mathbf{h}_n(t-\tau) b_n(\tau) d\tau \tag{8}$$

where $\mathbf{h}_n(t)$ is the inverse Fourier transform of $\mathbf{\Psi}_n(f)$. It can be seen that any two element processes from $\mathbf{p}_i(t)$ are statistically fully coherent, while any two processes from different $\mathbf{p}_i(t)$ and $\mathbf{p}_j(t)$ are non-coherent. Hence, each random process is viewed as a summation of mutually non-coherent component sub-processes.

The relationship between the eigenvectors of the covariance and frequency dependent eigenvectors of the XPSD matrices is:

$$\mathbf{\Phi \Omega \Phi}^T = \int_0^{\infty} \mathbf{\Psi}(f) \mathbf{\Lambda}(f) \mathbf{\Psi}^*(f) df \tag{9}$$

ANALYSIS OF WIND-INDUCED RESPONSE

Wind effects on structures can be conveniently separated into background and resonant components. Typically, the dynamic response analysis is conducted in modal space for computational efficiency. In general, while only a few number of modes need to be included for the resonant response, the background component requires larger number of modes. Therefore, direct calculation of the background response using quasi-static analysis enhances computational efficiency over the modal analysis approach. The background component of a specific response $y(z_0, t)$ (i.e. displacement, shear force, moment) and its mean square value can be given as:

$$y_b(z_0, t) = \mathbf{A p}(t) = \mathbf{A \Phi a}(t) \tag{10}$$

$$\sigma_{y_b}^2 = \mathbf{A R_p A}^T = \mathbf{A \Phi \Omega \Phi}^T \mathbf{A}^T = \sum_{n=1}^{N_R} c_n^2 \Omega_n \tag{11}$$

where $c_n = \sum_{j=1}^{N} A_j \Phi_{jn}$; $\mathbf{A}$ is the $1 * N$ influence vector; $\mathbf{p}(t)$ is the $N * 1$ external wind load vector; $\mathbf{a}(t)$ is the $N_R * 1$ expansion coefficient vector of POD; $\mathbf{\Phi}$ is the $N * N_R$ eigenvector matrix of the covariance matrix $\mathbf{R_p}$ of $\mathbf{p}(t)$; and N and N_R $(N_R \ll N)$ are the numbers of the discrete loads and the eigenvalues (wind load modes) considered, respectively.

Based on the load-response-correlation approach proposed by Kasperski (1992), the background component of the equivalent static load distribution for the peak response $y_{bmax} = g\sigma_{y_b}$ (where g is the peak factor) is expressed as:

$$\mathbf{F}_{eb} = g \mathbf{R}_p \mathbf{A}^T / \sigma_{y_b} = g \mathbf{\Phi \Omega \Phi}^T \mathbf{A}^T / \sigma_{y_b} = \sum_{n=1}^{N_R} c_n \Omega_n \mathbf{\Phi}_n / \sigma_{y_b} \tag{12}$$

It is noted that the background response and the associated equivalent static load can be expressed as a sum of the contribution from wind loading modes. The contribution of each mode depends on the influence function, loading mode shape and eigenvalue.

The resonant components can be calculated by using modal analysis technique. Considering the first q modes of the structural system, the equation of motion are reduced to q uncoupled equations in terms of the modal coordinates $\mathbf{X}(t)$. The XPSD matrix of $\mathbf{X}(t)$ is given by:

$$\mathbf{S_x}(f) = \mathbf{H}(f) \mathbf{\Theta}^T \mathbf{S_p}(f) \mathbf{\Theta H}^*(f) = \mathbf{D_x}(f) \mathbf{D_x}^*(f) \tag{13}$$

$$\mathbf{D_x}(f) = \mathbf{H}(f) \mathbf{\Theta}^T \mathbf{D}(f) \tag{14}$$

$$\mathbf{H}(f) = diag[H_j(f)]; \quad H_j(f) = 1/(m_j(-\omega^2 + \omega_i^2 + 2i(\xi_j + \xi_{aj})\omega_j\omega) \tag{15}$$

where $\mathbf{D}(f)$ is the $N_S * N_S$ decomposed matrix (Eq. 5, $N_s \ll N$). In the case of decomposition based on the eigenvectors of XSPD matrix, $\mathbf{D}(f) = \mathbf{\Psi}(f)\sqrt{\mathbf{\Lambda}(f)}$; $\mathbf{\Theta}$ is the $N * q$ structural natural modal shape matrix; $m_j, \omega_j = 2\pi f_j$ are the mass and frequency in j-th mode; ξ_j and ξ_{aj} are the structural and aerodynamic damping ratios in j-th mode ($j = 1, 2, ..., q$); and $i = \sqrt{-1}$.

The mean square value of j-th modal response is expressed as (Kareem 1999):

$$\sigma_{X_j}^2 = \int_0^\infty |H_j(f|^2 \mathbf{\Theta}_j^T \mathbf{S}_{\mathbf{P}}(f)\mathbf{\Theta}_j df = \sum_{n=1}^{N_S} \int_0^\infty |H_j(f)|^2 \chi_{jn}^2(f)\Lambda_n(f)df \tag{16}$$

where $\chi_{jn}(f) = \mathbf{\Theta}_j^T \mathbf{\Psi}_n(f)$. The resonant response component can be evaluated by assuming that the forcing function is placed by a white noise with a constant spectral density at the structural natural frequency (Kareem 1987):

$$\sigma_{X_{jr}}^2 = \sum_{n=1}^{N_S} \frac{\pi f_j \chi_{jn}^2(f_j)\Lambda_n(f_j)}{4(2\pi f_j)^4(\xi_j + \xi_{aj})m_j^2} \tag{17}$$

The resonant component of $y(z_0, t)$ is given by:

$$y_r(z_0, t) = \sum_{j=1}^{q} e_j X_{jr}(t); \quad \sigma_{y_r}^2 = \sum_{j=1}^{q} \sigma_{y_{jr}}^2 = \sum_{j=1}^{q} e_j^2 \sigma_{X_{jr}}^2 \tag{18}$$

where $e_j = \mathbf{A}\mathbf{M}_0\mathbf{\Theta}_j(2\pi f_j)^2$ is the participation coefficient of j-th mode to the response $y(z_0, t)$; and $\mathbf{M}_0$ is the mass matrix in physical coordinates. Accordingly, the j-th mode resonant equivalent static load distribution can be expressed in terms of inertial force distribution as:

$$\mathbf{F}_{erj} = g\mathbf{M}_0\mathbf{\Theta}_j(2\pi f_j)^2 \sigma_{X_{jr}} \tag{19}$$

It is noted that the resonant modal response and equivalent static load can be expressed as a sum of the components associated with frequency dependent loading modes. The contribution of each mode depends on the structural dynamic characteristics, loading mode shape and eigenvalue.

Alternatively, the background response can also be given in terms of modal responses. The mean square values of the background response in modal and physical coordinates are given by (Kareem 1999):

$$\sigma_{X_{jb}}^2 = \sum_{n=1}^{N_s} \frac{\int_0^\infty \chi_{jn}^2(f)\Lambda_n(f)df}{(2\pi f_j)^4 m_j^2} = \sum_{n=1}^{N_R} \frac{Q_{jn}^2 \Omega_n}{(2\pi f_j)^4 m_j^2}; \quad \sigma_{y_b}^2 = \sum_{j=1}^{q} \sigma_{y_{jb}}^2 = \sum_{j=1}^{q} e_j^2 \sigma_{X_{jb}}^2 \tag{20}$$

where $Q_{jn} = \mathbf{\Theta}_j^T \mathbf{\Phi}_n$.

The total absolute peak value of response $y(z_0, t)$ is then given by (Chen and Kareem 2000):

$$y_{max} = g\sigma_y = g\sqrt{\sigma_{y_b}^2 + \sigma_{y_r}^2} = g\left(\sigma_{y_b} W_b + \sum_{j=1}^{q} \sigma_{y_{jr}} W_{jr}\right) = \mathbf{A}\left(\mathbf{F}_{eb} W_b + \sum_{j=1}^{q} \mathbf{F}_{ejr} W_{jr}\right) \tag{21}$$

where W_b and W_{jr} are the weighting factors given by:

$$W_b = \sigma_{y_b}/\sigma_y; \quad W_{jr} = \sigma_{y_{jr}}/\sigma_y \tag{22}$$

Accordingly, the total equivalent static peak load distribution including static load $\mathbf{F}_s$ is given as:

$$\mathbf{F} = \mathbf{F}_s \pm \mathbf{F}_e = \mathbf{F}_s \pm (\mathbf{F}_{eb} W_j + \sum_{j=1}^{q} \mathbf{F}_{ejr} W_{jr}) \tag{23}$$

APPLICATION

A 76 story 306 meters with 76 DOF is used to discuss the formulation presented here. The first natural frequency and damping ratio are 0.160 Hz and 0.01, respectively. The mean wind velocity at height z_i above ground is given by the power law $U_i = U_{10}(z_i/10)^{0.4}$, where U_{10} is the mean wind velocity at 10 m above the ground and is chosen to be 15 m/sec. The one-sided cross-spectrum of along-wind fluctuation u_i and u_j $(i = 1, 2, ..., 76)$ is given by:

$$S_{u_i u_j}(f) = \frac{4k_0 U_{10}^2}{f} \frac{X^2}{(1+X^2)^{4/3}} coh(z_i, z_j, f) \tag{24}$$

$$coh(z_i, z_j, f) = \exp(-\frac{c_1 f |z_i - z_j|}{U_{10}}) \tag{25}$$

where X=$1200f/U_{10}$, k_0=0.03 and c_1=7.7

Based on the quasi-steady and strip theory, the drag on the i-th story is given by:

$$P_i(t) = 0.5\rho A_i C_D U_i^2 (1 + 2u_i(t)/U_i) \tag{26}$$

where drag coefficient C_D=1.2 and A_i is the tributary area for the i-th story unit. Figures 1 and 2 show the eigenvalues of the covariance matrix and the contribution of each loading mode to the background displacement at the top of the building. The total RMS response is given by the square root of the sum of the squares of each component. The loading mode shapes based on the covariance and XPSD matrices are shown in Fig. 3. The equivalent static load distributions (pressures) for the displacement at the top, the base shear force and base over-turning moment are shown in Fig. 6(b). Figure 6(a) also shows the mean static load (pressure) given by $\mathbf{F}_s$=$\{0.5\rho C_D U_i^2\}$. It is noted that the background response and loads are dominated by the first wind load mode. It contributed about 95%, 95% and 99% (i.e. $c_1^2\Omega_1 / \sum_{n=1}^{76} c_n^2 \Omega_n$) to the mean square displacement, base shear and base moment, respectively.

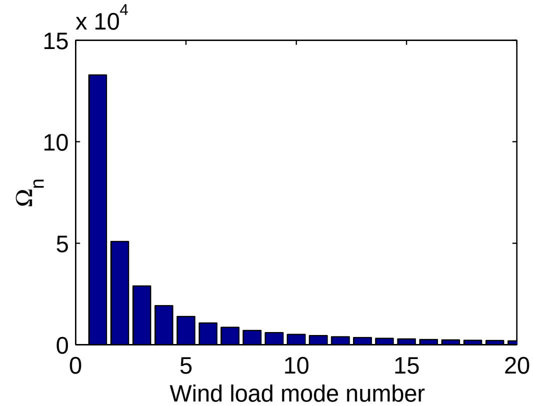

Fig. 1 Eigenvalues of covariance matrix

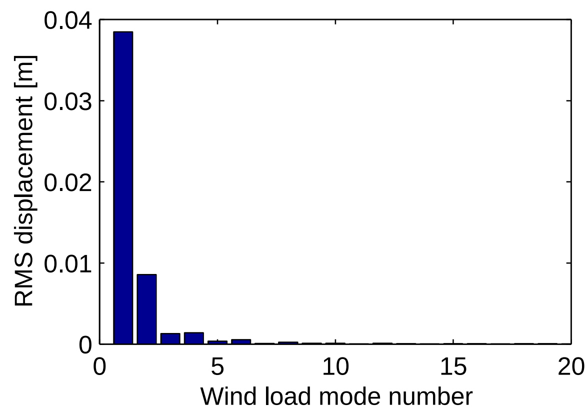

Fig. 2 Background displacement

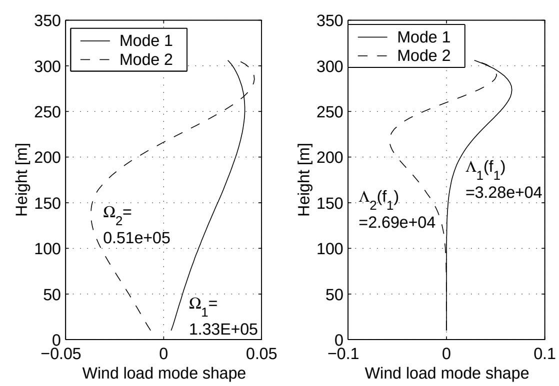

Fig. 3 Wind load mode shapes (a) from covariance matrix; (b) from XPSD matrix

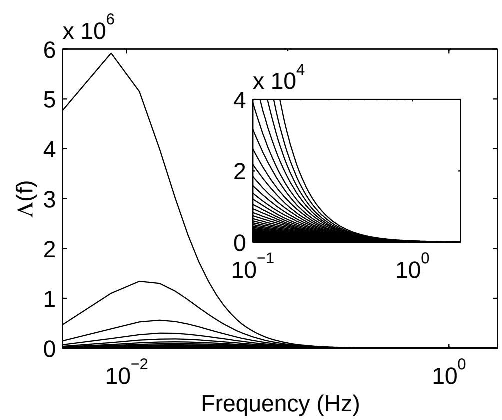

Fig. 4 Eigenvalues of XPSD matrix

Figure 4 shows the eigenvalues of the XPSD matrix at different frequencies. It is noted that at the lower frequency range the first wind load eigenvalue dominates, whereas at higher frequency range all the eigenvalues are of the same order. Figures 5(a) and 5(b) show $\chi_{jn}(f_i) = \mathbf{\Theta}_j^T \mathbf{\Psi}_n(f_i)$ (i=j=1,2; $n = 1, 2, ..., N_S$) which suggest relative significance of each loading mode to the first and second structural mode responses. These also show approximate orthogonality among loading modes and structural modes. Since the first loading mode shape is similar to the first structural mode, the orthogonality among the higher loading modes and first structural mode approximately holds. However, it is not true in the case of second structural mode, in which not only the first and second loading modes, but also the higher loading modes have non-negligible contribution. In fact, the loading modes depend on the spatial variation of the fluctuating wind field, these do not necessarily guarantee the orthogonality with the structural modes which depend on the mass and stiffness distribution of the structure. In this example, the RMS resonant response is dominated by the response in the first mode (more than 97%), which is contributed mainly by the first loading mode (about 90%). The ratios between mean square background and resonant responses are 0.32, 0.40 and 0.33 for displacement, base shear and base moment, respectively.

The resonant equivalent static loads for the first and second natural modes are shown in Fig. 6(c). The total peak equivalent static load is shown in Fig. 6(d). The peak factor g is assumed to be 3.5. The gust response factors for the displacement at the top of the building, base shear force and base over-turning moment are found to be 1.1124, 1.0384 and 1.0832, respectively.

The stochastic decomposition technique has been used in the simulation of random processes using spectral or hybrid spectral and time series schemes (Kareem 1999). It has also been implemented in state-space modeling of multi-correlated wind fields (Benfratello and Muscolino 1999; and Kareem and Mei 2000). The decomposition in Eq. 5 using modal scheme requires more computational effort in comparison

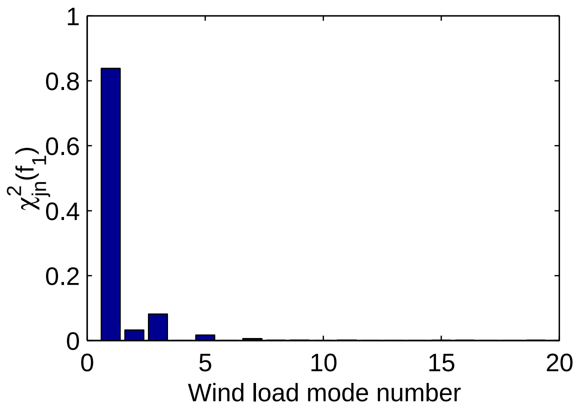

(a) First natural mode

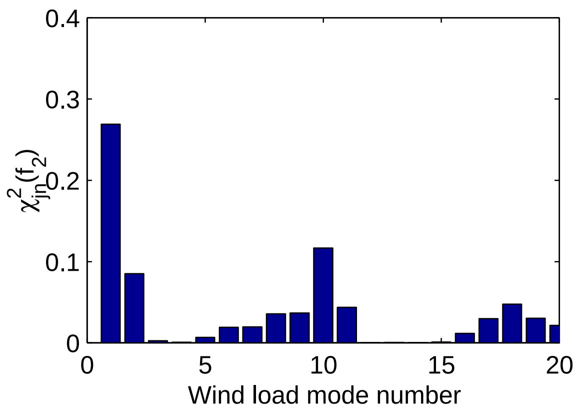

(b) Second natural mode

Fig. 5 Significance of loading modes to structural mode responses

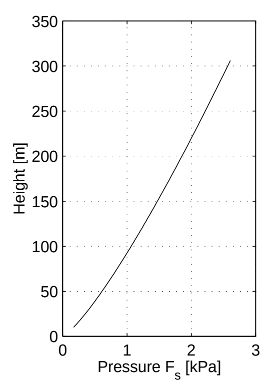

(a) Mean static load

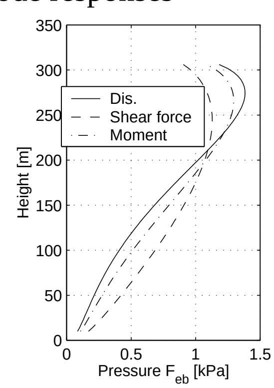

(b) Background load

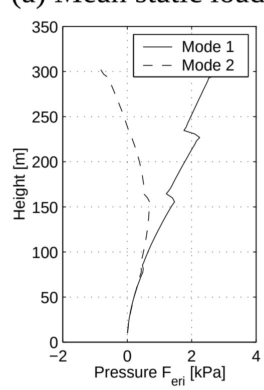

(c) Resonant load

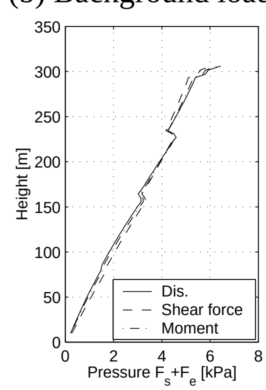

(d) Total load

Fig. 6 Equivalent static load distributions with the Cholesky decomposition. In both schemes, truncation of higher modes or reduction of the order of decomposition enhances computational efficiency. In the state-space modeling, further approximation of the frequency dependent eigenvectors of XPSD matrix is possible in special cases. The eigenvectors can be evaluated at a fixed frequency if the eigenvectors change very slowly with respect to the frequency (Kareem and Mei 2000).

Figure 7 shows the influence of the truncation of higher loading modes on the PSD of the generalized force in the first structural mode and of the force on the 50th story. The number of loading modes included is selected as 1, 2, 10 and 20. These reconstructed PSD are compared to the original untruncated. Results indicates that an accurate representation of the local element force, especially at higher frequency range, using the stochastic decomposition technique requires large number of loading modes, while only a few loading modes can accurately represent the global wind loads and their effects. The PSD in the high frequency range is particularly important for the estimate of resonant response of more flexible structure such as high-rise buildings.

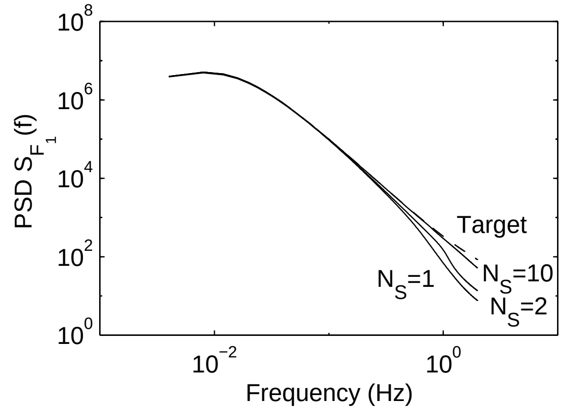

(a) Generalized modal force (mode 1)

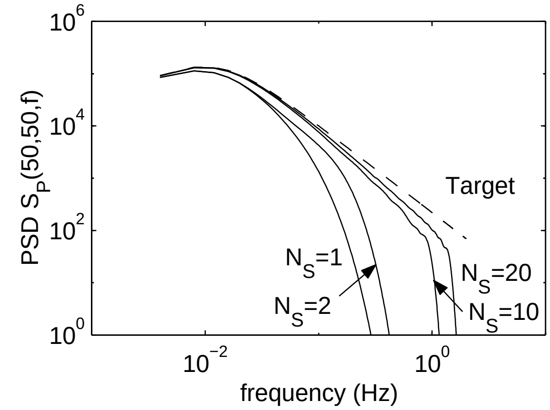

(b) Local forces on 50-th story

Fig. 7 Effects of higher mode truncation to PSD of rorces

From the coherence function of the wind field that decreases with the increase in frequency and spatial separation, it can be easily understood that at higher frequency range or with large spatial separation the wind fluctuations will become statistically non-coherent. Weakly coherent random fields require relatively large number of modes to be considered in the reconstruction. In the extreme case when the random processes are statistically non-coherent, i.e. the XPSD matrix is diagonal, all the modes will be needed for an accurate representation of the original random processe. Therefore, the efficiency and accuracy of these modeling and simulation techniques depends on the properties of the XPSD matrix and the frequency range of interest. The stochastic decomposition technique is especially very effective and efficient in simulating and modeling well correlated random fields such as the pressure fields around low-rise buildings, roofs and side faces of tall buildings.

CONCLUSIONS

Examining the wind load effects in light of the loading modes enhances our understanding of the dynamics of wind effects on structures. It also provides efficient way to estimate the background wind load effects, and serves as a useful tool for simulating and modeling multi-correlated wind fields by truncating higher modes. Results indicate that accurate representation of PSD at higher frequency range requires inclusion of larger number of modes, especially for local wind load effects.

ACKNOWLEDGMENTS

The support for this work was provided in part by NSF Grants CMS 9402196 and CMS 95-03779. This support is gratefully acknowledged.

REFERENCES

Amitt, J. (1968). Eigenvector analysis of pressure fluctuations on the west burton instrumented cooling tower. Central Electricity Research Laboratories, UK, Internal report RD/L/N 114/68.

Benfratello, S. and Muscolino, G. 1999. Filter approach to the stochastic analysis of MDOF wind-excited structures. *Prob. Engrg. Mech.*, 14, 311-321.

Bienkiewicz, B., Tamura, Y., Hann, H. J., Ueda, H. and Hibi, K. 1995. Proper orthogonal decomposition and reconstruction of multi-channel roof pressure. *J. of Wind Engrg. and Ind. Aerodyn.*, 54-55, 369-381.

Carassale, L., Piccardo, G. and Solari, G. 1998. Wind response of structures by double modal transformations. *Proc. of the 2nd East European Conference on Wind Engineering*, Prague, 7-11.

Chen, X., and Kareem, A. 2000. Equivalent static wind load distribution for coupled buffeting response of bridges, *Proc. of 8th ASCE Specialty on Prob. Mech. and Struct. Reliab.*, Notre Dame.

Davenport, A. G. 1995. How can we simplify and generalize wind loads? *J. of Wind Engrg. and Ind. Aerodyn.*, 54-55, 657-669.

Di Paolo, M. 1998. Digital simulation of wind field velocity. *J. of Wind Engrg. and Ind. Aerodyn.*, 74-76, 91-109.

Holmes, J. D. 1992. Optimized peak load distributions. *J. of Wind Engrg. and Ind. Aerodyn.*, 41-44, 267-276.

Kareem, A. 1978. Wind excited motion of buildings. Ph.D dissertation, Department of Civil Engineering, Colorado State University.

Kareem, A. 1987. Wind effects on structures: a probabilistic viewpoint. *Prob. Engrg. Mech.*, Vol.2, No.4, 166-200.

Kareem, A. 1999. Analysis and modelling of wind effects: numerical techniques. *Proc. of 10th Int. Conf. on Wind Engineering*, Copenhagen, 43-54.

Kareem, A. and Cermak, J. E. 1984. Pressure fluctuations on a square building model in boundary-layer flows. *J. of Wind Engrg. and Ind. Aerodyn.*, 16, 17-41.

Kareem, A., and Mei, G. 2000. Stochastic decomposition for simulation and modal space reduction in wind induced dynamics of structures. *Applications of Statistics and Probability*, Melchers & Stewart (eds), Balkema, Rotterdam, 757-764.

Kasperski, M. 1992. Extreme wind load distributions for linear and nonlinear design. *Engrg. Strut.*, 14, 27-34.

Lee, B. E. 1975. The effect of turbulence on the surface pressure field of a square prism. *J. of Fluid Mech.*, Vol.69, 263-282.

Li, Y. and Kareem, A. 1993. Simulation of multivariate random processes: a hybrid DFT and digital filtering approach. *J. of Engrg. Mech.*, ASCE, 119(5), 1078-1098.

Li, Y. and Kareem, A. 1995. Stochastic decomposition and application to probabilistic dynamics. *J. of Engrg. Mech.*, ASCE, 121(1), 162-174.

Lin, J. H. 1992. A fast CQC algorithm of PSD matrices for random seismic responses. *Computers and Structures*, Vol.44, No.3, 683-687.

Tamura, Y., Suganuma, S., Kikuchi, H. and Hibi, K. 1999. Proper orthogonal decomposition of random wind pressure field. *J. of Fluids and Struct.*, 13, 1069-1095.